Indian Journal of Pure & Applied Physics
Vol. 56, May 2018, pp. 383-391

Gamma, X-ray and neutron shielding properties of polymer concretes

L Seenappa[a,d], H C Manjunatha[a]*, K N Sridhar[b] & Chikka Hanumantharayappa[c]

[a]Department of Physics, Government College for Women, Kolar 563 101, India
[b]Department of Physics, Government First grade College, Kolar 563 101, India
[c]Department of Physics, Vivekananda Degree College, Bangalore 560 055, India
[d]Research and Development Centre, Bharathiar University, Coimbatore 641 046, India

Received 21 June 2017; accepted 3 November 2017

We have studied the X-ray and gamma radiation shielding parameters such as mass attenuation coefficient, linear attenuation coefficient, half value layer, tenth value layer, effective atomic numbers, electron density, exposure buildup factors, relative dose, dose rate and specific gamma ray constant in some polymer based concretes such as sulfur polymer concrete, barium polymer concrete, calcium polymer concrete, flourine polymer concrete, chlorine polymer concrete and germanium polymer concrete. The neutron shielding properties such as coherent neutron scattering length, incoherent neutron scattering lengths, coherent neutron scattering cross section, incoherent neutron scattering cross sections, total neutron scattering cross section and neutron absorption cross sections in the polymer concretes have been studied. The shielding properties among the studied different polymer concretes have been compared. From the detail study, it is clear that barium polymer concrete is good absorber for X-ray, gamma radiation and neutron. The attenuation parameters for neutron are large for chlorine polymer concrete. Hence, we suggest barium polymer concrete and chlorine polymer concrete are the best shielding materials for X-ray, gamma and neutrons.

Keywords: X-ray, Gamma, Mass attenuation coefficient, Polymer concrete

1 Introduction

Concrete is used for radiation shielding. Junior *et al.*[1] measured the mass attenuation coefficients of X-rays in different barite concretes. Malkapur *et al.*[2] evaluated the neutron radiation shielding characteristics of a polymer-incorporated self-compacting concrete mixes. Zorla *et al.*[3] studied the radiation shielding properties of high strength concrete containing varying fractions of natural and enriched boron. Cullu and Ertas[4] determined the radiation absorption capacity of concretes produced from lead mine wastes. Juncai *et al.*[5] established a model to predict the strength of radiation-shielding concretes. Yadollahi *et al.*[6] studied radiation shielding properties of concretes using artificial neural network. Singh *et al.*[7] reported the gamma radiation shielding properties of lead-flyash concretes. Fusco *et al.*[8] studied the shielding properties of protective thin film coatings on the blended concrete compositions. Alhajali *et al.*[9] studied different composition of concretes for nuclear reactor shielding. El-Sayed *et al.*[10] reported a comparative study of different concrete composition as gamma-ray shielding materials.

Agosteo *et al.*[11] studied the attenuation of secondary radiation in concretes. Maslehuddin *et al.*[12] studied the radiation shielding properties of concrete with heavyweight aggregates. Kharita *et al.*[13] investigated the effects of addition of boron compounds on the shielding properties of concretes. Yao *et al.*[14] studied the gamma ray shielding efficiency and mechanical performances of lead and bismuth based concretes. El-Khayatt[15] studied the gamma and neutrons shielding properties of lime/silica concretes. Ochbelagh and Azimkhani[16] studied the gamma-ray shielding properties of concrete containing different percentages of lead. Kharita *et al.*[17] prepared radiation shielding concretes using natural local materials. Pavlenko *et al.*[18] studied neutrons and gamma shielding properties of iron-barium concretes. Nemati *et al.*[19] measured the attenuation of neutrons in concretes. Pomaro *et al.*[20] studied the radiation damage in concrete shielding for nuclear physics experiments. Weinreich *et al.*[21] measured the accumulated uranium and plutonium content in concretes of nuclear reactor shielding. Singh *et al.*[22] measured the gamma radiation interaction parameters in flyash concretes. In our previous work[23-28], we have measured the X-ray and

*Corresponding author (E-mail: manjunathhc@rediffmail.com)

gamma interaction parameters in some compounds of dosimetric interest. We also reported theoretical studies on the X-ray and gamma interaction parameters of biological samples[29-32]. In our previous work[33], we have reported shielding parameters for beta and bremsstrahlung radiation in concretes.

In the present work, we have studied the X-ray and gamma radiation shielding parameters such as mass attenuation coefficient, linear attenuation coefficient, half value layer , tenth value layer, effective atomic numbers, electron density, exposure buildup factors, relative dose, dose rate and specific gamma ray constant in some polymer based concretes such as sulfur polymer concrete, barium polymer concrete, calcium polymer concrete, flourine polymer concrete, chlorine polymer concrete and germanium polymer concrete. It is also studied the neutron shielding properties such as coherent neutron scattering length, incoherent neutron scattering lengths, coherent neutron scattering cross section, incoherent neutron scattering cross sections, total neutron scattering cross section and neutron absorption cross sections in the polymer concretes.

2 Theory

2.1 Gamma/X-ray interaction parameters

In the present work, the mass attenuation coefficients (MAC) and photon interaction cross sections in the energy range from 1 keV to 100 GeV are generated using WinXCom[34] and its composition (Table 1). The total linear attenuation coefficient (μ) can be evaluated by multiplying density of compounds to mass attenuation coefficients:

$$\mu = \left(\frac{\mu}{\rho}\right)_c \times \rho \quad \ldots (1)$$

The total linear attenuation coefficient (μ) is used in the calculation of half value layer (HVL). HVL is the thickness of an interacting medium that reduces the radiation level by a factor of 2 that is to half the initial level and is calculated by the following equation:

$$\mathrm{HVL} = \frac{\ln 2}{\mu} = \frac{0.693}{\mu} \quad \ldots (2)$$

The total linear attenuation coefficient (μ) is also used in the calculation of tenth value layer (TVL). It is the thickness of interacting medium for attenuating a radiation beam to 10% of its radiation level and is computed by:

$$\mathrm{TVL} = \frac{\ln 10}{\mu} = \frac{2.303}{\mu} \quad \ldots (3)$$

The average distance between two successive interactions is called the relaxation length (λ). It is also called the photon mean free path which is determined by the equation:

$$\lambda = \frac{\int_0^\infty x \exp(-\mu x)dx}{\int_0^\infty \exp(-\mu x)dx} = \frac{1}{\mu} \quad \ldots (4)$$

Table 1 — Elemental composition of selected polymer based concrete

Element	Sulfur polymer concrete	Barium polymer concrete	Calcium polymer concrete	Flourine polymer concrete	Chlorine polymer concrete	Germanium polymer concrete
Na	0.18	0.18	0.18	0.18	0.18	0.18
Mg	0.15	0.15	0.15	0.15	0.15	0.15
Al	1.62	1.62	1.62	1.62	1.62	1.62
Si	15.71	15.71	15.71	15.71	15.71	15.71
P	0.12	0.12	0.12	0.12	0.12	0.12
S	24.3	-	-	-	-	-
Ba	-	25	-	-	-	-
Ca	-	-	25.33	-	-	-
F	-	-	-	25	-	-
Cl	-	-	-	-	25	-
Ge	-	-	-	-	-	25
K	0.27	0.27	0.27	0.27	0.27	0.27
Ca	0.33	0.33		0.33	0.33	0.33
Ti	0.19	0.12	0.12	0.12	0.12	0.12
Fe	0.55	0.55	0.55	0.55	0.55	0.55
H	18.86	18.65	18.65	18.65	18.65	18.65
C	18.86	18.65	18.65	18.65	18.65	18.65
O	18.86	18.65	18.65	18.65	18.65	18.65

The gamma interaction parameters such as linear attenuation coefficients, μ (cm^{-1}), HVL (in cm), TVL (in cm) and mean free path λ are calculated using above Eqs (1-4). The total molecular cross section σ_m [milli barn] is computed from the following equation using the values of mass attenuation coefficients[29-32] $[(\mu/\rho)_c]$:

$$\sigma_m(E) = \left(\frac{1}{N}\right)\left(\frac{\mu}{\rho}(E)\right)_c \sum_i n_i A_i \quad \ldots (5)$$

where n_i is the number of atoms of i^{th} element in a given molecule, $(\mu/\rho)_c$ is the mass attenuation coefficient of compound, N is the Avogadro's number and A_i is the atomic weight of element i. The effective (average) atomic cross section for a particular atom in the compound σ_a [milli barn] is estimated using the equation[29-32]:

$$\sigma_a(E) = \frac{\sigma_m}{\sum_i n_i} = \frac{\left(\frac{1}{N}\right)\left(\frac{\mu}{\rho}(E)\right)_c \sum_i n_i A_i}{\sum_i n_i} \quad \ldots (6)$$

The effective electronic cross section σ_e [milli barn] is computed from mass attenuation coefficient $(\mu/\rho)_i$ of i^{th} element in the given molecule using following equation[29-32]:

$$\sigma_e(E) = \left(\frac{1}{N}\right)\sum_i \left\{\left(\frac{f_i A_i}{Z_i}\right)\left(\frac{\mu}{\rho}(E)\right)_i\right\} \quad \ldots (7)$$

where f_i is the fractional abundance (a mass fraction of the i^{th} element in the molecule) and Z_i is the atomic number of the i^{th} element in a molecule. Finally the Z_{eff} is estimated as:

$$Z_{eff} = \frac{\sigma_a}{\sigma_e} \quad \ldots (8)$$

The effective electron density (N_e), expressed interms of number of electrons per unit mass is closely related to the effective atomic number. For an element, the electron density is given by

$N_e = NZ/A$ [electrons/g]. This expression can be generalized for a compound:

$$N_e(g^{-1}) = \frac{N}{\sum_i n_i A_i} Z_{eff} \sum_i n_i \quad \ldots (9)$$

2.2 Secondary radiation during the interaction of gamma/X-ray

During the interaction of gamma/X-ray with the medium, it degrades their energy and produces secondary radiations through the different interaction process. The quantity of secondary radiations produced in the medium and energy deposited/ absorbed in the medium is studied by calculating buildup factors. In the present work, we have estimated energy exposure build up factors (B_{en}) using GP fitting method[35-37]. We have evaluated the G-P fitting parameters (*b, c, a,* X_k and *d*) for different stent alloys using following expression which is based on Lagrange's interpolation technique:

$$P_{Z_{eff}} = \sum\left(\frac{\prod_{Z' \neq Z}(Z_{eff} - Z)}{\prod_{z \neq Z}(z - Z)}\right) P_z \quad \ldots (10)$$

where lower case z is the atomic number of the element of known G-P fitting parameter P_z adjacent to the effective atomic number (Z_{eff}) of the given material whose G-P fitting parameter $P_{Z_{eff}}$ is desired and upper case Z are atomic numbers of other elements of known G-P fitting parameter adjacent to Z_{eff}. GP fitting parameters (*b, c, a,* X_k and *d*) for element adjacent to Z_{eff} are provided by the standard data available in literature[38]. The computed G-P fitting parameters (*b, c ,a,* X_k and *d*) were then used to compute the EABF in the energy range 0.015 MeV-15 MeV up to a penetration depth of 40 mean free path with the help of G-P fitting formula, as given by the equations[35-37]:

$$B(E,X) = 1 + \frac{b-1}{K-1}(K^X - 1) \text{ for } K \neq 1 \quad \ldots (11)$$

$$B(E,X) = 1 + (b-1)X \text{ for } K=1 \quad \ldots (12)$$

$$K(E,X) = CX^a + d\frac{\tanh(\frac{X}{X_K} - 2) - \tanh(-2)}{1 - \tanh(-2)} \text{ For penetration depth } (X) \leq 40 \text{ mfp} \quad \ldots (13)$$

where X is the source-detector distance for the medium in mean free paths (mfp) and b is the value of build-up factor at 1mfp. K (E,X) is the dose multiplication factor and *b, c ,a,* X_k and *d* are computed G-P fitting parameters that depend on attenuating medium and source energy.

2.3 Relative dose

The radial dependence of dose is exp $(-\mu r)B/r^2$, where μ denotes the linear attenuation coefficient for the appropriate photon energy and B is the exposure build-up factor. Dose distribution at a distance r is given by[36]:

$$D_r = D_0 e^{-\mu \times r}\, B/r \qquad \ldots (14)$$

Here D_0 is the initial dose delivered by the point gamma ray emitter. The relative dose distribution at a distance r is:

$$\frac{D_r}{D_0} = e^{-\mu \times r}\, B/r \qquad \ldots (15)$$

Hence the relative dose distribution can be evaluated using estimated exposure build-up for different penetration depths.

2.4 Specific gamma ray constant

Specific gamma ray constant (Γ) is an exposure rate (in R/h) due to photons at a distance of one meter from a source with an activity[39] of 1Ci:

$$\Gamma = \frac{E_\gamma\left(\frac{\text{MeV}}{\text{decay}}\right)\times\left(1.6\times10^{-13}\,\frac{\text{J}}{\text{MeV}}\right)\times\left(\frac{\mu_{en}}{\rho}\,\frac{\text{cm}^2}{\text{g}}\right)\times\left(3600\,\frac{\text{sec}}{\text{hr}}\right)\times\left(3.7\times10^{10}\,\frac{\text{Bq}}{\text{Ci}}\right)}{4\pi\left(34\,\frac{\text{J}}{\text{kg}}/\frac{\text{C}}{\text{kg}}\right)\times\left(100\,\frac{\text{cm}}{\text{m}}\right)^2\times\left(2.58\times10^{-4}\,\frac{C}{\text{kg}}/R\right)\times\left(10^{-3}\,\frac{\text{kg}}{\text{g}}\right)\times\left(\text{Bq}/\frac{\text{decay}}{\text{sec}}\right)}$$

$$\Gamma = 657.68\times E_\gamma\left(\frac{\mu_{en}}{\rho}\right)\frac{R\bullet m^2}{Ci\bullet hr} \qquad \ldots (16)$$

Specific gamma ray constant for given gamma energy is calculated by substituting μen/ρ from Eq. (4).

2.5 Dose and dose rate

Dose (D) and dose rate (D_{rate}) at a distance r and time t from a source of activity A are represented by following equations:

$$D = \frac{\Gamma C t}{r^2} \qquad \ldots (17)$$

$$D_{\text{rate}} = \frac{\Gamma C}{r^2} \qquad \ldots (18)$$

$$D_{\text{rate}} = \dot{\psi}\left(\frac{\mu_{en}}{\rho}\right) = \frac{CE}{4\pi r^2}\left(\frac{\mu_{en}}{\rho}\right) \qquad \ldots (19)$$

Here $\dot{\psi}$ is energy fluence rate (MeV/cm^{2}s), C is Activity in Bq, E is energy per decay (MeV). (μ_{en}/ρ) is mass energy absorption coefficient.

2.6 Neutron shielding parameters

The neutron shielding properties $(\text{NSP})_{\text{concrete}}$ such as coherent neutron scattering length, incoherent neutron scattering lengths, coherent neutron scattering cross section, incoherent neutron scattering cross sections, total neutron scattering cross section and neutron absorption cross sections in the polymer concretes are calculated using following mixture rule:

$$(\text{NSP})_{\text{concrete}} = \sum f_i (\text{NSP})_i \qquad \ldots (20)$$

Here $(\text{NSP})_i$ is neutron shielding parameter of i^{th} element[40] in the concrete and f_i is the fractional abundance (a mass fraction of the i^{th} element in the molecule). From the computed neutron cross sections, attenuation parameter of neutron is evaluated using the relation:

$$\text{attenuation parameter} = \frac{\sigma \times N_A}{A}\ \text{cm}^2/\text{g} \qquad \ldots (21)$$

where N_A and A are Avogadro number and atomic weight, respectively. σ is evaluated cross section in barn.

3 Results and Discussion

The elemental composition considered for different polymer concretes are as shown in Table 1. Literature survey[41] reveals that the sulfur polymer concrete with 25% of sulfur is proved to be a good thermoplastic and sustainable material. Polymer concrete up to 25% of barium is proved as good durability and resistance to salts, acids, and other corrosive materials[42]. Similarly we have chosen the fractions of the elements in the concrete and it is shown in Table 1. The calculated mass attenuation coefficient values for different polymer based concretes in the energy range 1 keV-100 GeV are shown in Fig. 1. Mass attenuation coefficient values for polymer concretes are large in the low energy region and decreases, progressively. In the low energy region, mass attenuation coefficient is

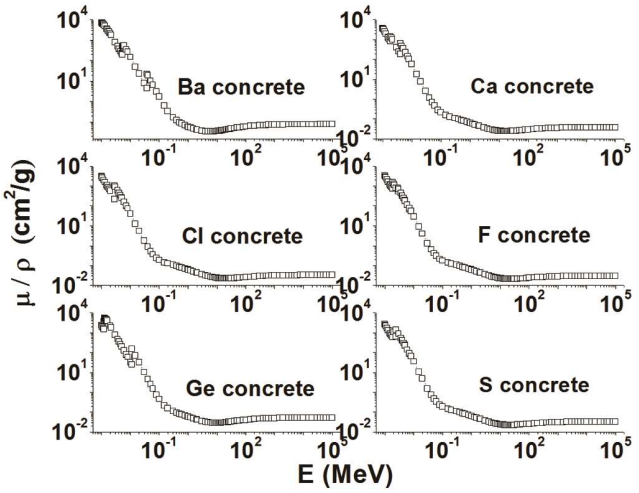

Fig. 1 — Variation of mass attenuation coefficient with energy for different polymer concretes.

observed to be high due to the dominant photoelectric interaction. In the high energy region, Compton scattering becomes dominent which depends linearly with atomic number. Hence, mass attenuation coefficient value becomes minimum value.

We have also calculated the half value layer, tenth value layer and mean free path for different polymer concretes. The comparision of half value layer, tenth value layer and mean free path for different polymer concretes are as shown in Fig. 2. From this comparison, it is clear that the half value layer, tenth value layer and mean free path are small for barium polymer concrete than the other polymer concretes. It means gamma/X-ray penetrates less in barium polymer concrete than the other polymer concretes.

The variation of effective atomic number and electron density with energy for different polymer concretes are as shown in Figs 3 and 4. These parameters for polymer concretes are large in the low energy region (due to photo electric effect) and decrease progressively, there after increases and becomes constant for high energy (due to pair production). The variation of energy exposure buildup factor (EBF) for polymer concretes are as shown in Fig. 5. It is observed that EBF increases up to the E_{pe} and then decreases. Here E_{pe} is the energy value at which the photo electric interaction coefficients matches with Compton interaction coefficients for a given value of effective atomic number (Z_{eff}). The variation of exposure buildup factors with mean free path at various energies (0.1, 0.5, 1.5, 5 and 15 MeV) for different polymer concretes are as shown in Fig. 6. From this figure it is clear that EBF values increases with increase in the target distance. This is due to the reason that with increase in the target distance, scattering events in the medium increases. Figure 7 shows the variation of relative dose with energy at variuos mean free paths (λ=1, 5, 10, 20 and 40) and target distance r=0.5 m for different polymer concretes. Figure 8 shows that the variation of relative dose with the energy at various target distances (r=0.1, 0.2, 0.5 and 1m) and at mean free path λ= 40 for different polymer concretes. From the Figs 7 and 8, it is clear that relative dose of gamma and X-ray increases with increase in the energy, mean free path and target distance.

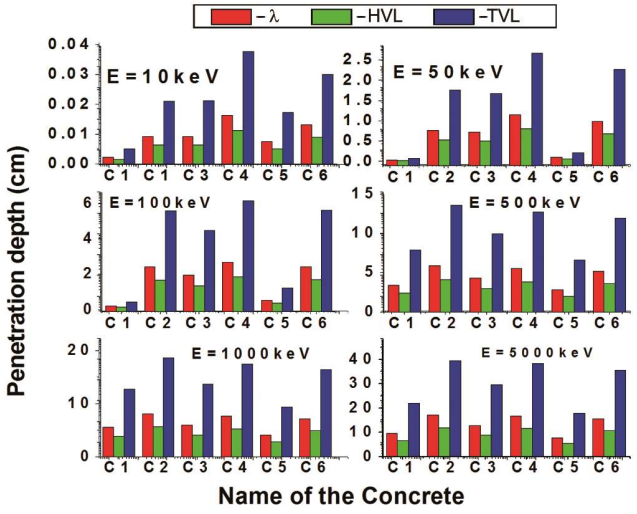

Fig. 2 — Comparison of half value layer (HVL),tenth value layer (TVL) and mean free path (λ) for different polymer concretes (C1-Barium Polymer concrete, C2-Calcium Polymer concrete, C3- Chlorine polymer concrete,C4-Flourine polymer concrete, C5- Germanium polymer concrete and C6-Sulfur polymer concrete).

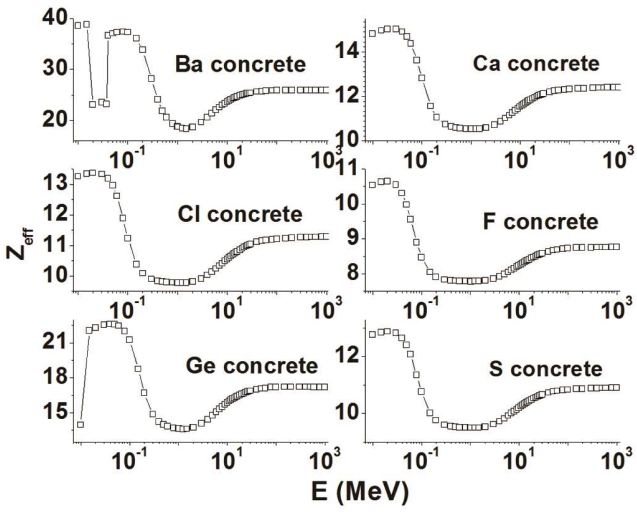

Fig. 3 — Variation of effective atomic number with energy for different polymer concretes.

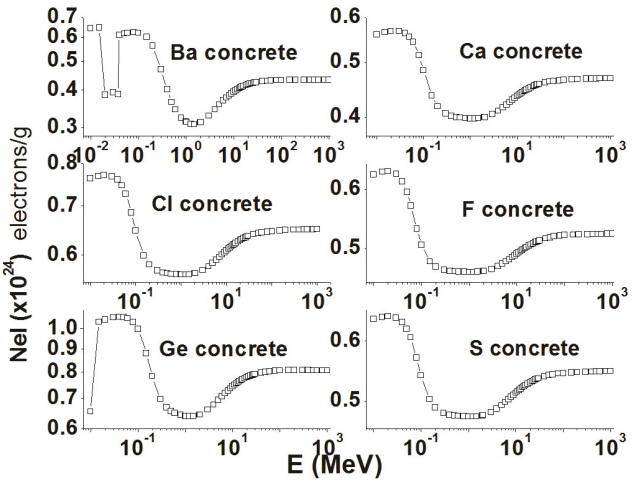

Fig. 4 — Variation of effective electron density with energy for different polymer concretes.

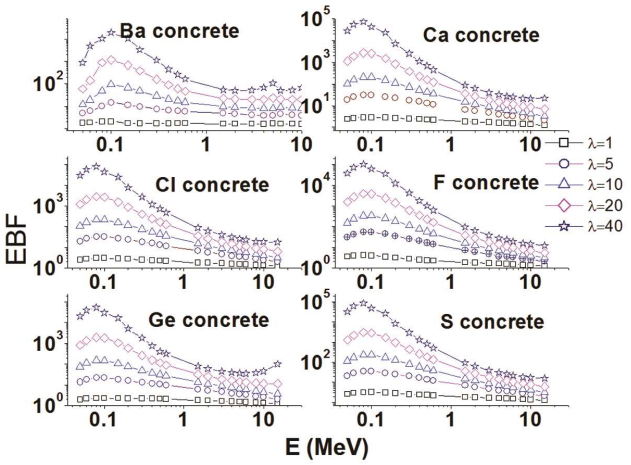

Fig. 5 — Variation of exposure buildup factors with energy for different polymer concretes.

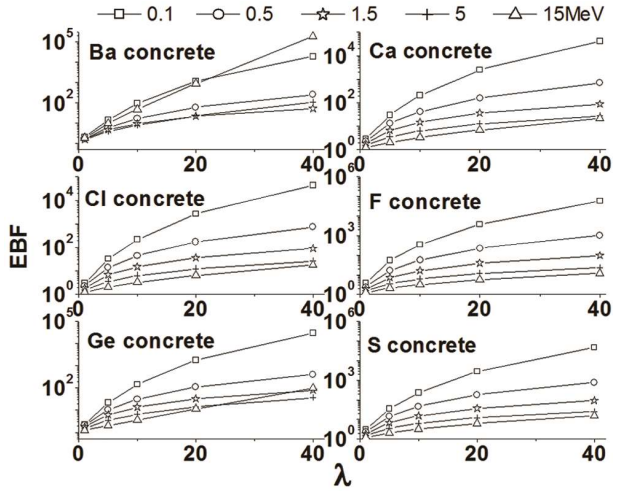

Fig. 6 — Variation of exposure buildup factors with mean free path at different energies for different polymer concretes.

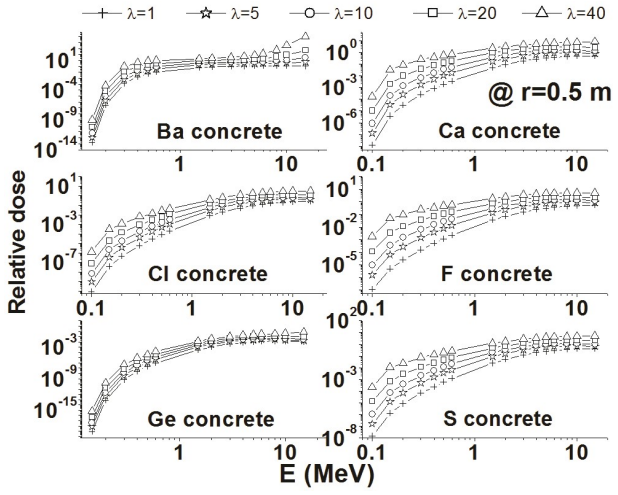

Fig. 7 — Variation of relative dose with energy at variuos mean free paths (λ=1, 5, 10, 20 and 40) and target distance *r*=0.5 m for different polymer concretes.

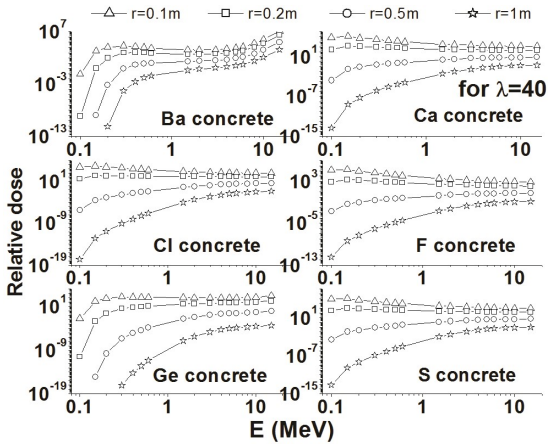

Fig. 8 — Variation of relative dose with energy at variuos target distances (*r*=0.1, 0.2, 0.5 and1 m) and at mean free path λ= 40 for different polymer concretes.

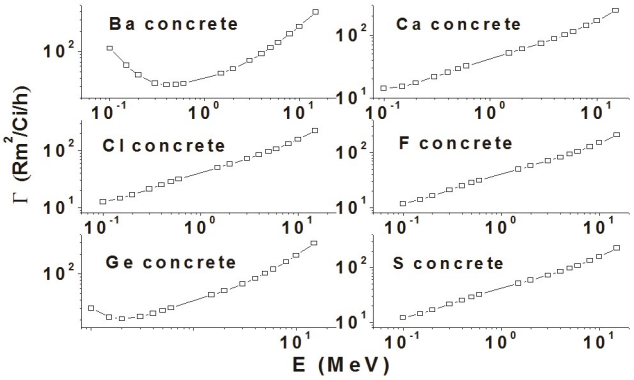

Fig. 9 — Variation of specific gamma ray constant with energy for different polymer concretes.

Figure 9 shows the variation of specific gamma ray constant with energy for different polymer concretes. The comparison of specific gamma ray constant for different polymer concretes is shown in Fig. 10. This comparison shows that specific gamma ray constant is large for barium polymer concrete than the other polymer concretes. This specific gamma ray constant is an exposure rate (in *R*/*h*) due to photons at a distance of one meter from a source of activity 1Ci. Figure 11 shows the variation of dose rate (*R*/*hr*) of gamma/X-ray with thickness of the medium for different polymer concretes. The dose rate of gamma/X-ray decreases with increase in the thickness of the medium.

The evaluated neutron attenuation parameters (cm^2/g) for different process in polymer concretes are givend in the Table 2. From this table, it is clear that the total neutron attenuation parameter for absorption and scattering is maximum for chlorine polymer

Table 2 — Neutron attenuation parameters (cm^2/g) for different process in polymer concretes

Concrete type	Coherent	In coherent	Absorption	Total
Sulfur polymer concrete	1.459E-04	7.737E-06	1.599E-05	1.536E-04
Barium Polymer concrete	2.928E-05	7.615E-08	2.043E-04	2.935E-03
Calcium Polymer concrete	1.101E-04	1.261E-06	1.263E-05	1.113E-04
Flourine polymer concrete	2.421E-04	3.265E-06	2.064E-05	2.453E-04
Chlorine polymer concrete	3.762E-04	8.392E-05	2.419E-05	4.608E-04
Germanium polymer concrete	4.653E-05	1.349E-05	5.873E-06	6.026E-05

Table 3 — Comparison of calculated mass attenuation coefficients (cm^2/g) with that of experiments

Energy (keV)	Ordinary concrete				Barium concrete	
	Experimental	Geant 4	Fluka	Present work	Experimental	Present work
48	-	-	-	0.340	1.47[43]	5.078
59.5	0.231[46]	-	0.234[46]	0.249	-	3.75
65		-	-	0.241	0.75[43]	1.74
80	–	-	0.184[46]	0.204	-	0.979
83	-	-	-	0.194	0.45[43]	0.386
118	-	-	-	0.163	0.23[43]	0.228
356	0.081[46]	-	0.094[46]	0.100	-	0.103
511	-	-		0.088	0.0918[44]	0.071
662	0.095 [44]	-		0.079	0.075[44]	0.072
1173.2	0.058[46]	-	0.055[46]	0.059	-	0.074
1332.5	0.051[46]	-	0.051[46]	0.055	-	0.074
1500	0.164[45]	0.141[45]	-	0.053	-	0.074
2000	0.116[45]	0.112[45]	-	0.045	-	0.075
3000	0.099[45]	0.089[45]	-	0.037	-	0.075
4000	0.087[45]	0.082[45]	-	0.032	-	0.076
5000	0.078[45]	0.062[45]	-	0.029	-	0.076
6000	0.078[45]	0.074[45]	-	0.026	-	0.076

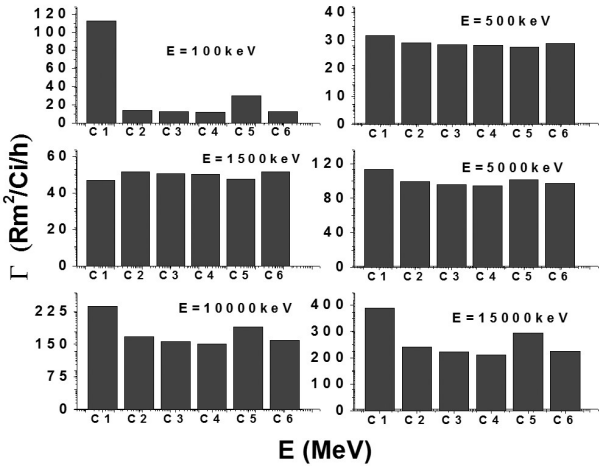

Fig.10 — Comparison of specific gamma ray constant for different polymer concretes. (C1-Barium Polymer concrete, C2-Calcium Polymer concrete, C3-Chlorine polymer concrete,C4-Flourine polymer concrete, C5- Germanium polymer concrete and C6-Sulfur polymer concrete).

concrete. The comparison of evaluated coherent neutron scattering length, incoherent neutron scattering lengths, coherent neutron scattering cross section, incoherent neutron scattering cross sections,

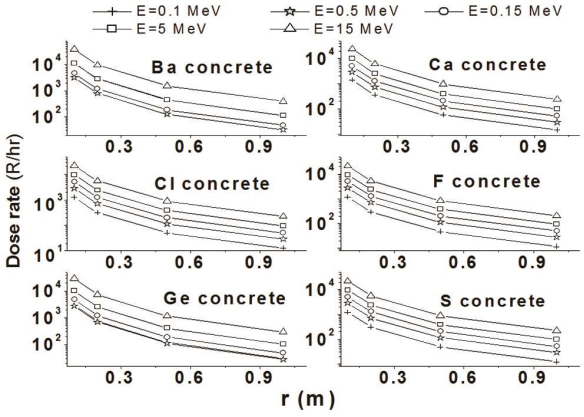

Fig. 11 — Variation of dose rate of gamma/X-ray with distance for different polymer concretes.

total neutron scattering cross section and neutron absorption cross sections for different polymer concretes are as shown in Fig. 12. From this figure, it is clear that coherent neutron scattering length and incoherent neutron scattering lengths are maximum for chlorine polymer concrete. Coherent, incoherent and total neutron scattering cross sections are large for chlorine polymer concrete. The neutron absorption

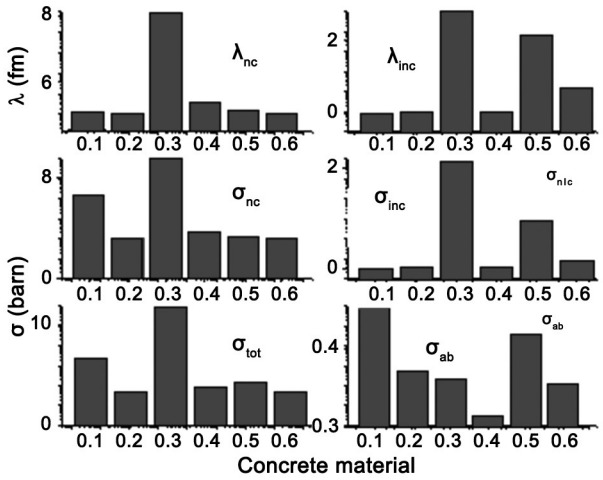

Fig. 12 — Comparison of evaluated coherent neutron scattering length (λ_{nc}), incoherent neutron scattering lengths (λ_{inc}), coherent neutron scattering cross section (σ_{nc}), incoherent neutron scattering cross sections (σ_{inc}), total neutron scattering cross section (σ_{tot}) and neutron absorption cross sections (σ_a) for different polymer concretes (C1-Barium Polymer concrete, C2-Calcium Polymer concrete, C3-Chlorine polymer concrete,C4-Flourine polymer concrete, C5- Germanium polymer concrete and C6-Sulfur polymer concrete).

cross section is high for barium polymer concrete. To validate the present calculation, we have compared the computed mass attenuation coefficients with that of the experiments. Table 3 shows the comparison of calculated mass attenuation coefficients (cm^2/g) with that of experiments.

4 Conclusions

We have studied the X-ray, gamma and neutron shielding parameters in polymer concretes. From the detail study, it is clear that barium polymer concrete is good absorber for X-ray, gamma radiation and neutron. The attenuation parameters for neutron are large for chlorine polymer concrete. Hence, we suggest barium polymer concrete and chlorine polymer concrete are best shielding materials for X-ray, gamma and neutrons.

References

1 Junior A, Nogueira M S, Vivolo V, Potiens M P A & Campos L L, *J Radiat Phys Chem*, 02 (2017) 054.
2 Malkapur M, Divakar L, Narasimhan M C, Karkera N B, Goverdhan P, Sathian V & Prasad N K, *Appl Radiat Isotopes*, 125 (2017) 86.
3 Zorla E, Ipbüker C, Biland A, Kiisk M, Kovaljov S, Tkaczyk A H & Gulik V, *Nucl Eng Design*, 313 (2017) 306.
4 Cullu M & Ertas H, *Constr Build Mater*, 125 (2016) 625.
5 Juncai X, Ren Q & Zhenzhong S, *Ann Nucl Energy*, 85 (2015) 296.
6 Yadollahi A, E Nazemi, Zolfaghari A & Ajorloo A M, *Prog Nucl Energy*, 89 (2016) 69.
7 Singh K, Singh S, A Dhaliwal S & Singh G, *Appl Radiat Isotopes*, 95 (2015) 174.
8 Fusco A, Winfrey L, Mohamed A & Bourham, *Ann Nucl Energy*, 89 (2016) 63.
9 Alhajali S, Yousef S & Naoum B, *Appl Radiat Isotopes*, 107 (2016) 29.
10 Waly E S A, Mohamed A & Bourham, *Ann Nucl Energy*, 85 (2015) 306.
11 Agosteo S, Mereghetti A, Sagia E & Silari M, *Nucl Instr Meth Phys Res B*, 319 (2014) 154.
12 Maslehuddin M, Naqvi A, Ibrahim M & Kalakada Z, *Ann Nucl Energy*, 53 (2013) 192.
13 Kharita M H, Yousef S & Nassar M A, *Prog Nucl Energy*, 53 (2011) 207.
14 Yao Y, Zhang X, Li M & Yang R, *Radiat Phys Chem*, 127 (2016) 188.
15 El-Khayatt A M, *Ann Nucl Energy*, 37 (2010) 991.
16 Rezaei-Ochbelagh D & Azimkhani S, *Appl Radiat Isotopes*, 70 (2012) 2282.
17 Kharita M H, Takeyeddin M, Alnassar M & Yousef S, *Prog Nucl Energy*, 50 (2008) 33.
18 Pavlenko V I, Yastrebinskii R N & Voronov D V, *J Eng Phys Thermophys*, 81 (2008) 686.
19 Nemati M J, Habibi M & Amrollahi R, *J Radioanal Nucl Chem*, 295 (2013) 221.
20 Pomaro B , V Salomoni A, Gramegna F, Prete G & Majorana C E, *Ann Solid Struct Mech*, 2 (2004) 123.
21 Weinreich R, Bajo S, Eikenberg J & Atchison F, *J Radioanal Nucl Chem*, 261 (2004) 319.
22 Singh K, Singh S, Singh S P, Mudahar G S & Dhaliwal A S, *J Radiol Prot*, 35 (2015) 2.
23 Manjunatha H C, *Radiat Phys Chem*, 113 (2015) 24.
24 Seenappa L, Manjunatha H C, Chandrika B M & Chikka H, *J Radiat Prot Res*, 42 (2017) 26.
25 Manjunatha H C, *Radiat Phys Chem*, 137 (2016) 254.
26 Manjunatha H C, Seenappa L, Chandrika B M & Chikka H, *Ann Nucl Energy*, 109 (2017) 310.
27 Rudraswamy B, Dhananjaya N & Manjunatha H C, *Nucl Instr Meth Phys Res Sec A*, 619 (1) (2010) 171.
28 Manjunatha H C, Chandrika B M, Seenappa L & Chikka H, *Int J Nucl Energy Sci Technol*, 10 (2016) 356.
29 Manjunatha H C & Rudraswamy B, *Health Phys*, 104 (2013) 158.
30 Suresh K C, Manjunatha H C & Rudraswamy B, *Radiat Prot Dosim*, 128 (2008) 294.
31 Manjunatha H C & Rudraswamy, *Health Phys*, 100 (2011) S92.
32 Manjunatha H C, *J Med Phys*, 39 (2014) 112.
33 Manjunatha H C, Chandrika B M, Rudraswamy B & Sankarshan B M, *Nucl Instr Meth Phys Res Sec A*, 674 (2012) 74.
34 Gerward L, Guilbert N, Jensen K B & Levring H, *Radiat Phys Chem*, 71 (2004) 653.
35 Manjunatha H C & Rudraswamy B, *Radiat Measure*, 47(5) (2012) 364.
36 Manjunatha H C & Rudraswamy B, *Radiat Phys Chem*, 80 (2011) 14.
37 Manjunatha H C & Rudraswamy B, *J Radioanal Nucl Chem*, 294 (2) (2012) 251.
38 American National Standard (ANS), (1991) ANSI/ANS 643.
39 Manjunatha H C, *Pramana J Phys*, 89 (2017) 42.
40 Sears V F, *Neutron News*, 3 (2006) 26.

41 Moon J, Kalb P D, Milian L & Northrup P A, *Cem Concr Compos*, 67 (2016) 20.
42 Espeland J D, Espeland R W & Olson M L, United States Patent: US006034155A.
43 Almeida J T, Nogueira M S, Santos M A P, Campos L L & Araujo F G S, *Radiat Phys Chem*, (2017) 02054.
44 Stankovic, Ilic R D, Jankovic K, Bojović D& Lončar B, *Acta Physica Polonica A*, 117 (2010).
45 Singh P, Medhat M E & Badiger N M, *J Radioanal Nucl Chem*, 300 (2014) 325.
46 Gurler & Akar T, *J Radioanal Nucl Chem*, 293 (2012) 397.